Molecular and Cellular Biochemistry (2025) 480:3765–3781
https://doi.org/10.1007/s11010-025-05216-z

# PAX2 induces endometrial cancer by inhibiting mitochondrial function via the CD133—AKT1 pathway

**Fu Hua**[1,2] · **YunLang Cai**[1]

Received: 20 September 2024 / Accepted: 22 January 2025 / Published online: 1 February 2025


## Abstract

Endometrial cancer (EC) is a malignancy of the endometrial epithelium. The prevalence and mortality rates associated with the disease are on the rise globally. A total of 20 cases of type I EC tissues were collected for transcriptomic sequencing, our findings indicate that PAX2 is highly expressed in EC tissues and is closely related to the pathogenesis of EC. PAX2 is a member of the paired homeobox domain family and has been linked to the development of a number of different tumours. In normal endometrial tissue, PAX2 is methylated; however, in EC, it is demethylated. Nevertheless, few studies have focused on its role in EC. A protein–protein interaction (PPI) analysis revealed a regulatory relationship between PAX2 and CD133, which in turn affects the activity of AKT1. CD133 is a well-known marker of tumor stem cells and is involved in tumor initiation, metastasis, recurrence, and drug resistance; AKT1 promotes cell survival by inhibiting apoptosis and is considered a major promoter of many types of cancer. Nevertheless, further investigation is required to ascertain whether PAX2 affects the progression of EC by regulating the CD133-AKT1 pathway. The present study demonstrated that PAX2 promoted cell proliferation, migration, invasion and adhesion, and inhibited apoptosis. Its mechanism of action was found to be the inhibition of mitochondrial oxidative phosphorylation, promotion of glycolysis, increase in mitochondrial copy number, and increase in the levels of reactive oxygen species (ROS) and hexokinase, as well as the concentration of mitochondrial calcium ions. This was achieved through the promotion of CD133 expression and the phosphorylation of AKT1. In conjunction with the aforementioned regulatory pathways, the progression of EC is facilitated.

**Keywords** Endometrial cancer · PAX2 · CD133 · Tumor initiation · Mitochondrial function

## Introduction

Endometrial cancer (EC) is a prevalent gynecological malignancy, with the majority of cases occurring between the ages of 65 and 75 [1]. The 5-year survival rate for EC patients is estimated at 81% (67% of whom are identified in the early stages), yet the survival rate for stage IVA and stage IVB EC is only 17% and 15%, respectively [2], which demonstrate the significance of ethnic, socioeconomic, and geographic differences in terms of morbidity and mortality. Research has revealed a correlation between an augmented risk of EC and age, ethnicity, BMI, estrogen exposure (intravenous or exogenous), tamoxifen use, premature menarche, late menopause, parity reduction, metabolic syndrome, family history, and genetic susceptibility [3]. In contrast, lower EC risk is associated with normal BMI, higher parity, and oral contraceptive use [4]. The etiology and pathogenesis of EC remain obscure, yet a considerable amount of Type I EC is linked to estrogen. Research found that estrogen receptors (ER) α, ERβ and progesterone receptors (PR) bind to specific response elements during ligand interactions and regulate target genes involved in growth and differentiation. Many ERα gene targets have been identified as key genes induced by estradiol and/or tamoxifen and promoting EC cell growth, such as insulin-like growth factor 1 (IGF1), c-myc, and PAX2 [5, 6]. Currently, EC is considered to be a reproductive endocrine disease with numerous inducible factors, limited therapeutic methods, and no targeted drugs, most studies have focused on general tumor pathogenesis

✉ YunLang Cai
caiyl2021@163.com

[1] Department of Obstetrics and Gynecology, Zhongda Hospital, School of Medicine, Southeast University, No.87 Dingjiaqiao, Nanjing 210009, China

[2] Department of Gynecology, the Affiliated Huaian No. 1 People's Hospital of Nanjing Medical University, Huai'an, Jiangsu, China

signaling pathways, therefore, it is of great significance to research the targeted molecules and pathways for the treatment of EC.

Studies have shown that PAX2 plays an important role in organ formation during embryonic development [7]. PAX2 is highly expressed in kidney tumor [8], EC [9], ovarian cancer [10], breast cancer [11], prostate cancer [12] and other tumor tissues. PAX2 has also been identified as a target for transcriptional suppression of the tumor suppressor gene WT1 [13]. Tamoxifen was found to activate transcription of the ER target gene PAX2 in endometrial cells. PAX2 has also been shown to be essential in the proliferative response of steroid hormones and tamoxifen in EC and has been identified as a key gene in estradiol and/or tamoxifen induction [14]. It has been reported that PAX2 is methylated in normal endometrial, but demethylated in EC [6]. At present, it has been confirmed that PAX2 is correlated with the occurrence of a variety of tumors, PAX2 expression levels are different in different types of EC, the role of PAX2 in the pathogenesis of EC remains to be further studied. Protein–protein interaction (PPI) was used to analyze the regulatory genes related to PAX2, and it was suggested that PAX2 was related to prominin 1(*prom1*), but the regulatory relationship is unclear. The *prom1* gene is known to encode a five-transmembrane glycoprotein that is a membrane-organizing extension spike protein, which is expressed in adult stem cells and is thought to maintain stem cell characteristics by inhibiting differentiation. The *prom1* gene encodes a protein commonly known as CD133, which has been found to be expressed in cancer stem cells from prostate, lung, brain, colon, ovarian cancer, and acute lymphoblastic leukemia. Studies have found that endometrial CD133 + tumor cells show the characteristics of cancer stem cells [15]. Thus, our study investigated whether PAX2 contributes to the pathogenesis and progression of EC by regulating CD133 expression and the underlying mechanism.

Studies indicated that when cells are unable to generate sufficient energy through mitochondria, up-regulation of oncogene and down-regulation of tumor suppressor gene occurs to maintain glycolysis, and at the same time a large body of evidence suggests that mutant cancer phenotypes are associated with impaired mitochondrial function and that normal mitochondrial function suppresses tumourigenesis [16]. A complex interaction between AKT1 (also known as Protein Kinase B α) and mitochondrial dysfunction has been identified. AKT1 is a serine/threonine protein kinase belonging to the Akt family, which responds to a variety of stimuli such as hormones, growth factors and extracellular matrix components in cells [17]. It is involved in glucose metabolism, transcription, cell survival, proliferation, angiogenesis and cell motility, and is involved in a variety of biological processes such as tumour development [18]. The present study thus sought to ascertain whether PAX2 affects mitochondrial function by regulating the CD133-AKT1 pathway, thereby influencing the development of EC.

## Materials and methods

### Sample collection

In order to gain insight into the underlying mechanisms of EC, a total of 40 tissue samples were collected, comprising 20 normal human endometrial tissues and 20 human EC tissues. Endometrial cancer patient samples are retained in three portions of approximately 100 mg of tissue each. The patient's tumour tissue is surgically removed and sent for pathology testing. Following the results of the pathology tests, which confirm the presence of adenocarcinoma of the endometrium, the patient's tissue is included in the pool of samples to be tested. Normal endometrial tissue is obtained from discarded tissue scrapings taken from patients without endometrial tumours. These patients may present with a range of menstrual disorders or may have other conditions such as uterine polyps. Following the pathological diagnosis of the normal endometrial tissue, three portions of 100 mg each were included in the experimental study sample bank. Ensuring that experiments involving humans have been conducted in accordance with The Code of Ethics of the World Medical Association (Declaration of Helsinki), all patients have signed informed consent and acquired ethical qualifications. Inclusion criteria: age 50–65 years, female, no hormone therapy in the past three months, excluding patients with non-endometrioid carcinoma (clear cell carcinoma and serous adenocarcinoma) and patients receiving preoperative chemotherapy.

### RNA extraction and transcriptomic sequencing

Fresh tissue is used for RNA extraction in this study. After vigorous shaking with chloroform (200 µl, Sinopharm, China) for 30 s, the tissues in the eppendorf (EP) tubes were homogenized using Trizol (ThermoFisher, USA). The EP tube was kept at 4 °C for 15 min, followed by a centrifuge at 12,000 rpm for the same duration. Subsequently, the supernatant of the liquid was transferred to a new RNA-free EP tube, and 500 µl of isopropyl alcohol was added to each tube and blended well. Finally, the EP tube was kept at 4 °C for 10 min and centrifuged at 12,000 rpm. After 10 min, a white sediment was discovered at the bottom of the EP tube, and the supernatant was discarded. Subsequently, 75% ethanol was used to wash RNA precipitation, and the RNA precipitation was kept at room temperature for desiccation. After the DEPC $H_2O$ had dissolved the RNA, transcriptome sequencing was conducted to determine its quality and

concentration (Personalbio Technology Co. Ltd., China). The samples were initially subjected to total RNA extraction. Following this, target RNA enrichment was conducted, after which transcriptome libraries were constructed and quantified. The libraries were then sequenced using Illumina sequencing methods. Data comparisons and calculations of gene expression levels of the filtered sequences were conducted. The online tool DAVID was employed to perform functional enrichment and pathway enrichment analysis of the differentially expressed genes (DEGs) among three groups, while STRING database was utilized for PPIs analysis of the DEGs.

## Real-time PCR

According to the analysis results of DEGs, real-time PCR was used to verify the top 10 high level and low level DEGs. At first, reverse transcription reaction is performed to reverse RNA to cDNA for fluorescence quantitative PCR reaction. 20 µl reaction system of TAKARA's TB Green Premix Ex Taq II (Tli RNaseH Plus) kit was used. Using GAPDH as an internal reference, the following procedure was employed to perform a two-step PCR amplification: 95 °C for 1 min (1 cycle), 95 °C for 5 s, 60 °C for 1 min (45 cycles), and stored at 4 °C. The results were then analyzed using the $2^{-\Delta\Delta CT}$ method. The necessary primers are listed in Table 1.

## Western blot assay

BCA protein quantification (Beyotime, China) was performed for every tissue and cell lysate before western blot assay. Electrophoresis with SDS-PAGE was employed to separate proteins, which had been transferred to a PVDF membrane (Millipore, USA). Blocking liquid (Beyotime, China) was then used to block nonspecific protein at room temperature for 30 min. Rabbit primary antibody CD133 (1:1000, CST, USA) and mouse primary antibody β-actin (1:5000, CST, USA) were then added to the membrane and incubated at 4 °C with a gradual shaking process overnight. After washing the PVDF membrane 3 times with washing buffer for 15 min, a secondary antibody (goat anti-rabbit, 1:2000, CST; goat anti-mouse, 1:2000, CST; USA) was incubated at room temperature for 2 h. Subsequently, chemiluminescence detection was conducted using ECL working solution (Beyotime, China). The PVDF membrane was then placed on the gel imager (Thermo Scientific, USA), and the imaging time was adjusted to the depth of the displayed band. Image J software was used to measure the gray value and quantitatively analyzed.

**Table 1** The primers of top 10 high level and low level DEGs

| Gene (high) | Forward primer | Reverse primer |
|---|---|---|
| *Pax2* | TGTCAGCAAAATCCTGGGCAG | GTCGGGTTCTGTCGTTTGTATT |
| *Itgad* | TCCCATCGTCCAACTGAAAGG | TGTACTTCTGCCCATCTGTGAT |
| *Ascl1* | CCCAAGCAAGTCAAGCGACA | AAGCCGCTGAAGTTGAGCC |
| *Chd5* | GCCCGTGAGCCTTCCTAAG | GGGGAGTAGTCACTGCCTTC |
| *Hpse2* | ATGGCCGGGCAGTAAATGG | GCTGGCTCTGGAATAAATCCG |
| *Znf717* | GCCAACTTGCTGTAGAAAGTCT | GGCATCTTGCACTGTAGCATAAG |
| *Adgra2* | CCCTACGCCAAGTGGTGTTC | GAAGGTGCAGTCGTGGATGAG |
| *Arhgap20* | GACTACCCGAAGAGCATTCCC | AGAGCCAGTTATCCCTAGCATT |
| *Gli2* | CTGCCTCCGAGAAGCAAGAAG | GCATGGAATGGTGGCAAGAG |
| *Cor2b* | CGTCCGCAATACCGTAGCTC | TAGTTGGGTTCAATCCTGCCT |
| Gene (low) | Forward primer | Reverse primer |
| *Spink1* | TCTATCTGGTAACACTGGAGCTG | ACACGCATTCATTGGGATAAGT |
| *Calml5* | GGTTGACACGGATGGAAACG | ACTCCTGGAAGCTGATTTCGC |
| *Jsrp1* | TGTCGCTCAACAAGTGCCTG | GCCTGGGCCTCGAACTTAG |
| *Krt6a* | GAAAATGGCGAGTTTTACGA | CGCGTCTCCTAAACCTTCGG |
| *Sim2* | CCATTTAGGCTTATCCCAGGTG | GGTCATCTCATCGTGGTCAGA |
| *Pitx2* | CGGCAGCGGACTCACTTTA | GTTGGTCCACACAGCGATTT |
| *S100a2* | GCCAAGAGGGCGACAAGTT | AGGAAAACAGCATACTCCTGGA |
| *Fam83a* | GGCCCTAAGGGACTGGACT | CACAGTGGCGCTGGATTTTT |
| *Tff3* | CCAAGCAAACAATCCAGAGCA | GCTCAGGACTCGCTTCATGG |
| *C4bpb* | TCTGCAAAAGTAGGGACTGTGA | CACGCCCACTAAGTAGTACCT |

## Immunohistochemical staining and immunofluorescence staining

Immersing paraffin sections of human normal endometrial and EC tissue in xylene I (Beyotime, China) for 20 min and then rinsing with tap water, the slices were then put into various concentrations of ethanol (Beyotime, China) to hydrate and rinsed with tap water for a further 20 min. After hydration, the slice was placed on a metal slice rack and putted it into a beaker containing sodium citrate antigen repair solution (Beyotime, China) and heated at 95 ℃ for 15 min. After 0.01 M PBS (Beyotime, China) had been washed through the slices, the tissues were incubated with blocking solution (Beyotime, China) at room temperature for 30 min. Subsequently, rabbit PAX2 antibodies (CST, USA), CD133 antibodies (CST, USA) were diluted 1:100 in the dilution, mixed, and dropped onto the tissue's surface. The tissue was then incubated at 4° C overnight, and washed with 0.01 M PBS for 10 min, 3 times. The SV hypersensitive two-step histochemical kit (rabbit/mouse IgG) (Boster, China) was employed for immunohistochemical staining. Subsequent to the addition of polyclonal HRP-labeled anti-rabbit/mouse IgG, the slices were incubated at 37 °C for 30 min, followed by a PBS rinse for 5 min × 3 times. Subsequently, DAB staining, hematoxylin re-staining, dehydration, and transparent and neutral gum sealing were performed. After incubation of the primary antibody, fluorescent secondary antibody labeling is necessary for immunofluorescence staining. The Goat anti-rabbit 555 secondary antibody (Invitrogen, USA) was incubated at 37 °C for 1 h at room temperature, then washed with 0.01 M PBS for 10 min, repeated three times. DAPI staining solution (Beyotime, China) was added dropwise on the tissue section, the coverslips were covered. The staining situation was observed under a light field or fluorescence field microscope (Olympus, Japan). A statistical analysis of immunohistochemistry and immunofluorescence staining was conducted between groups using the ImageJ software.

## Enzyme-linked immunosorbnent assay

An enzyme-linked immunosorbent assay (ELISA) kit was employed to examine the expression of PAX2 (COIBO, China), CD133 (COIBO, China) and phospho-AKT1 (Abcam, USA) in 40 human tissues, 4 tumor tissues derived from BALB/c-nu mice and HEC-A cells. The specific experimental steps are in accordance with the instructions provided in the kit. Briefly, the standard and sample wells should be set up, and the samples to be tested should be diluted with the provided sample diluent. Subsequently, the sample is to be added to the lower portion of the wells within the plate, with 100 µl of enzyme reagent to be added to each well, with the exception of the wells designated as blanks. The plate should then be sealed with sealing film and incubated at 37 °C for a period of 60 min. The sealing film should be removed with great care, after which the liquid should be discarded, the wells shaken dry, and washing solution added. This process should be repeated five times, with a 30-s waiting period between each addition and removal of the solution. Subsequently, 50 µl of colour developer A and then 50 µl of colour developer B should be added to each well, shaken gently and mixed well. The colour should then be developed at 37 °C for 15 min. Finally, 50 µl of termination solution should be added to the wells to terminate the reaction. The reaction should be zeroed with a blank well, and the absorbance (OD) of each well should be measured sequentially at 450 nm.

## Luciferase reporter assay

HEC-1A cells (Cell Bank, Shanghai Institute for Biological Science, Shanghai, China) were inoculated in 6-well plates at a density of approximately 50% of the maximum inoculum density. The Lipofectamine 2000 Reagent was employed to facilitate the transfection of cells in the designated groups with 3 µg of the pGL6-CMV-Luc blank vector plasmid, the pGL6-CMV-Luc-CD133 plasmid (CD133 wild type, inclusive of the CD133 gene promoter region) and the pGL6-CMV-Luc-CD133 mutant plasmid (CD133 mutant, characterised by a deletion mutation of 'GCAGTGAACCAT GATTA' in the promoter region). At 72 h post-transfection, the dual-luciferase reporter assay system (Beyotime China) was employed to quantify luciferase activity in each experimental group. The corresponding value of fluorescence emitted by the firefly luciferase-inducible substrate (FL) and fluorescence released by the renilla luciferase-inducing substrate (RL) was determined utilising a microplate reader. Subsequently, the ratio of the value of FL to RL was determined for each sample, which was then taken as the relative luciferase activity of the reporter gene.

## Tumour formation assay in nude mice

In order to observe the effect of PAX2 on the development of EC, we used a PAX2 adenoviral interference plasmid to infect HEC-1A cells. Following this, a stable interfering cell line was obtained, and the cells were inoculated in the logarithmic growth phase in the dorsal subcutaneous area of 6-week-old BALB/c-nu mice. Nude mice were inoculated with $5 \times 10^5$ cells in a volume of 0.2 ml. The presence of a subcutaneous mass was measured weekly, the size of the tumour was measured weekly, and after one month, the tumour tissue was taken for volume and weight measurements for intergroup comparisons. Tumour tissues were subsequently used for further experiments for preservation.

### Cell proliferation assay and cell adhesion assay

The CCK-8 assay kit (Beyotime, China) is employed to identify cell proliferation or adhesion. 96-well plates were seeded with HEC-1A cells ($1 \times 10^4$ cells/well), which were then subjected to PAX2 or CD133 interference, as well as a negative control plasmid (control), or addition of the PAX2 inhibitor EG1 (MCE, USA). To assess whether PAX2 promotes the emergence of EC by CD133, recombinant human PAX2 protein was utilized. Cells were incubated about 24 h with or without laminin, 20 µl CCK-8 were added into the cells incubated at 37 °C for 4 h. A microplate reader (Molecular devices, USA) was used to analyze the cell proliferation or growth rate to determine the absorbance at 450 nm.

### Transwell assay

Chemotactic migration of HEC-1A cells was measured using a transwell chamber (Corning Inc. USA) with a 6.5 mm polycarbonate membrane (pore size 8 µm). HEC-1A cells ($5 \times 10^4$ cells/well) which were interfered with PAX2 or CD133 or negative control plasmid (control), or addition of the PAX2 inhibitor EG1 (MCE, USA) with DMEM + 5% fetal bovine serum (FBS) (Gibco, USA) was seeded on the upper chamber, followed by DMEM + 10% FBS in the lower chamber. Afterward, the cells were incubated for approximately 24 h in the cell incubator (Thermofisher, USA). To eliminate any non-migrating cells on the upper surface of the polycarbonate membrane, a cotton swab was employed. Subsequently, they were fixed with 4% paraformaldehyde for 15 min and stained with crystal violet at room temperature for 10 min. A bright field microscope was used to count the number of cells that migrate to the sub-membrane surface and take the average value (randomly select 10 fields), the assay was to observe the migration of EC cells after interfering with PAX2 or CD133 and/or with recombinant human (rh) PAX2 (10 ng/µl, abcam, USA).

### Wound-healing assay

Using the wound-healing assay, the migratory ability of HEC-1A cells was measured. In brief, 6-well plates were seeded with HEC-1A cells and grown to 90% confluency. A 20 µl pipette tip was used to create a scratch, and an image was taken straight away. After 24 h of incubation at 37 °C, the images were taken again and the migration of the cells was randomly calculated by counting those that had moved above the reference line. The control group was calculated as 100 and the experimental group compared with the control group to ascertain the difference between the groups.

### Tunel assay

After discarding the culture solution, cells were then fixed with 4% paraformaldehyde for 15 min. Subsequently, PBS containing 0.3% triton X-100 (Beyotime, China) was added to the cells and incubated at room temperature for 5 min. Finally, 50 µl TUNEL detection solution (Beyotime, China) was added to the cells and left to incubate in the dark at 37 °C for 60 min, the cells were observed with a fluorescence microscope after mounting with anti-fluorescence quenching mounting solution.

### The oxygen consumption rate (OCR) and extracellular acidification rate (ECAR) assay

Cells were inoculated in seahorse-specific 96-well culture plates, rh CD133 (100 ng/µl, abcam, USA) and rh PAX2 (10 ng/µl, abcam, USA) were added to cell culture supernatants 24 h before the assay. Appropriate experimental conditions were selected, the reaction drugs were added sequentially according to OCR and ECAR requirements, and cellular oxygen consumption and acidification rate were detected using the Seahore XFp Analyzer (Agilent, USA), respectively.

### Mitochondrial DNA (mtDNA) copy number detection assay

Initially, the cell samples underwent whole-genome extraction using the Genome Extraction Kit (ThermoFisher, USA). The mtDNA copy number quantification was performed using the Human Mitochondrial DNA Copy Number Quantification qPCR Assay Kit (ScienCell Research Laboratories, USA), according to the manufacturer's protocols. For each genomic DNA sample, prepare two qPCR reactions, one with mtDNA primer stock solution, and one with human single copy reference (SCR) primer stock solution. 20 µl qPCR reaction system (per sample): 1 µl DNA template (5 ng/L), 2 µl mtDNA, 10 µl 2 X GoldNStart TaqGreen qPCR master mix, 7 µl RNAase-free H2O. Initial denaturation at 95 °C for 10 min was followed by 32 cycles of denaturation at 95 °C for 20 s, annealing at 52 °C for 20 s, and extension at 72 °C for 45 s. For mtDNA, ΔCq (mtDNA) is the quantification cycle number difference of mtDNA between the target and the reference genomic DNA samples. $2^{-\Delta\Delta Cq}$ was used to calculate relative mtDNA copy number of the target sample to the reference sample (fold). AKT1 agonist SC79 (10 µM) (MCE, USA) and AKT1 antogonist Capivasertib (5 µM) (MCE, USA) was used to detect the role of AKT1 in regulating mitochondrial DNA levels.

### ROS detection assay

Cellular ROS content was measured using a ROS assay kit (Beyotime, China). Briefly, cells were inoculated in 96-well plates ready for fluorescence detection, the cell culture medium was removed and the appropriate volume of diluted DCFH-DA was added. The cells were incubated for 20 min at 37 °C in a cell culture incubator. The cells were washed three times with serum-free cell culture medium to adequately remove DCFH-DA. The fluorescence intensity was detected before and after stimulation using an activation wavelength of 488 nm and an emission wavelength of 525 nm. The active oxygen content in each group was calculated by utilizing the positive control and fluorescence density values provided in the kit. AKT1 agonist SC79 (10 μM) (MCE, USA) and AKT1 antogonist Capivasertib (5 μM) (MCE, USA) was used to detect the role of AKT1 in regulating ROS levels.

### Mitochondrial calcium ion concentration detection assay

To measure the concentration of calcium ions in mitochondria, we extracted the cellular mitochondria (Beyotime, China). Briefly, the cells were digested and collected using pancreatic enzyme cell digestion fluid, they were then washed with PBS and then 1.5 ml of mitochondrial separation reagent was added. The cells were kept at 4 °C for 15 min. The cells were homogenised and then centrifuged at 600 g for 10 min at 4℃. The supernatant was transferred to another centrifuge tube and centrifuged at 11,000 g for 10 min at 4 °C. The precipitate is the isolated cellular mitochondria. Following the instructions on the calcium test kit (Merck, USA), the OD value at 610 nm was read using a microplate reader (ThermoFisher, USA) and the mitochondrial calcium content of the target cells was calculated based on the formula. AKT1 agonist SC79 (10 μM) (MCE, USA) and AKT1 antogonist Capivasertib (5 μM) (MCE, USA) was used to detect the role of AKT1 in regulating mitochondrial calcium ions levels.

### Hexokinase detection assay

Hexokinase is the first key enzyme in glucose catabolism, catalysing the conversion of glucose to glucose 6-phosphate, and glucose 6-phosphate dehydrogenase further catalysing the dehydrogenation of glucose 6-phosphate to form NADPH. NADPH has a characteristic absorption peak at 340 nm. The experiments were conducted following the instructions provided by the hexokinase assay kit (Nanjing jiancheng, China). The cells were collected through centrifugation at 600 g for 5 min at 4 °C. They were then washed with 10 mL of ice-cold PBS and centrifuged again at 600 g for 5 min at 4 °C. Finally, the supernatant was removed. 1 ml of extract buffer was added to the precipitate, followed by ultrasonic cell-breaking at 4 °C. The resulting mixture was then centrifuged at 8000 g for 10 min at 4 °C, and the supernatant was collected. The concentration of hexokinase was determined by measuring the OD value at 340 nm using a microplate reader (ThermoFisher, USA) and calculating it according to the assay instructions. AKT1 agonist SC79 (10 μM) (MCE, USA) and AKT1 antogonist Capivasertib (5 μM) (MCE, USA) was used to detect the role of AKT1 in regulating mitochondrial hexokinase levels.

### Statistical analysis

All experiments in this study were repeated 6 times or more. Using SPSS 18.0 software, the experimental data were statistically analyzed. The mean ± SD of the measurement data were expressed, and the mean of two independent samples was compared using a *t* test. Analysis of variance was used to compare data between multiple groups, with $P < 0.05$ indicating a statistically significant difference.

## Results

### Transcriptomic sequencing of human normal endometrium (NE) and endometrial carcinoma (EC) tissues to identify differentially expressed genes

In order to identify genes that are differentially expressed, RNA sequencing was performed on normal endometrial tissue and endometrial cancer tissue. Figure 1A and B illustrate the DEGs identified through the aforementioned methods and the associated significance thresholds. Compared to the NE group, the EC group exhibited 807 up-regulated genes and 792 down-regulated genes. The circle map of the genome, which is based on genomic information and differential RNA expression analysis, provides an illustration of the distribution of differentially expressed genes on chromosomes between NE and EC tissues (Fig. 1C). The DEGs were subjected to functional enrichment analysis using GO and KEGG pathway analyses. The results of these analyses are presented in Fig. 1D and E. Additionally, the following heat-map illustrates the relative expression levels of PAX2, CD133 and other differential genes, highlighting significant disparities in expression between the two groups and their association with the development of endometrial cancer (Fig. 1F). The analysis of transcriptomic data from normal and EC tissue is a key step in our research, as it allows us to identify key genes that regulate endometrial cancer pathogenesis. Following the DEGs analysis, the ten genes with the highest and lowest expression levels were selected for verification using a real-time PCR assay. The results confirmed

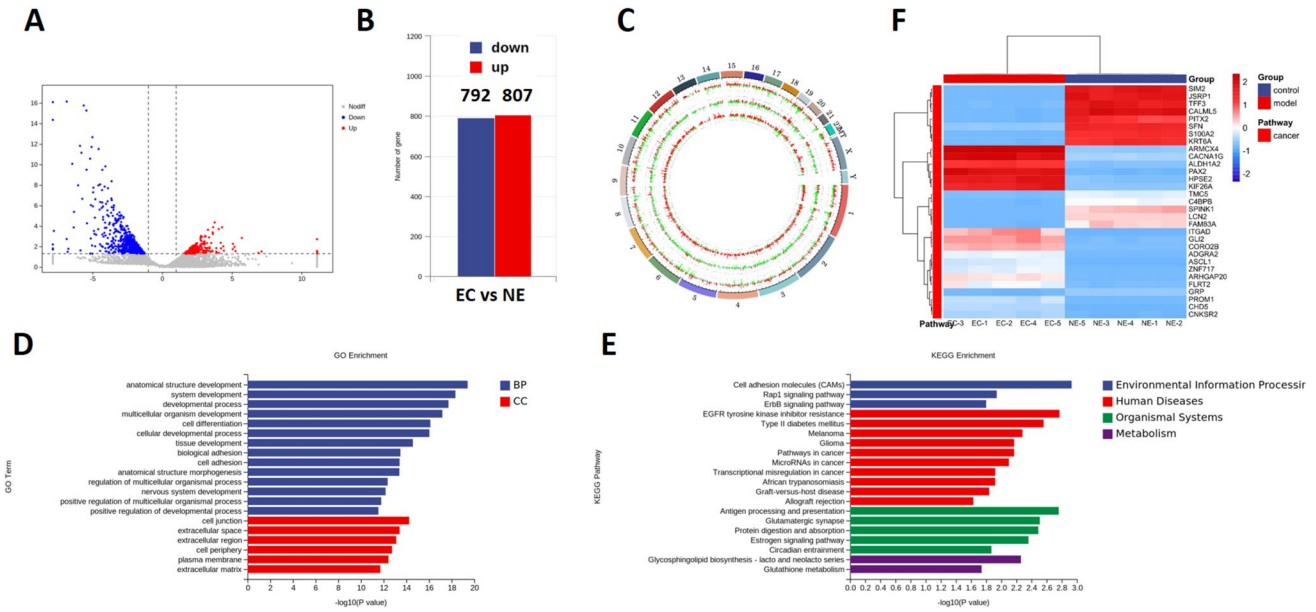


**Fig. 1** Transcriptomic sequencing of normal endometrium (NE) and human endometrial carcinoma (EC). **A** The volcano map showed the differentially expressed genes (DEGs) of NE group and EC group, the colour blue indicates genes that are down-regulated in comparison to the NE group, whereas the colour red indicates genes that are up-regulated. **B** Compared with NE group, EC group had 792 down-regulated genes and 807 up-regulated genes. **C** The genomic circle map reflects the distribution of differential genes on chromosomes between NE tissue and EC tissue. **D** GO analysis indicates the presence of altered functional genes that are associated with processes related to cell development, differentiation and adhesion. **E** KEGG analysis has revealed DEGs in the cell adhesion molecule pathway, the EGFR pathway and the estrogen pathway, which are associated with tumour growth. **F** A heat-map is used to show where there is a difference in the genes that are associated with the development of EC

the expression of the top-ranked gene, PAX2 (Fig. 2A and B), it is proposed that PAX2 may play a significant role in the development of EC. In order to analyse the mechanisms by which PAX2 regulates the pathogenesis of endometrial cancer in depth, the PAX2 PPI network (Fig. 2C) was subjected to analysis using GO functional enrichment and KEGG pathway enrichment discovery. This analysis revealed the potential involvement of PAX2 in endometrial cancer, with the hypothesis being that it exerts its regulatory influence on the PROM1 gene.

### *Expression of PAX2 and its target genes CD133 in* human *EC tissues*

To validate the results of RNA sequencing, immunohistochemical methods were employed to detect PAX2 expression in EC. The results demonstrated that PAX2 expression was increased in EC tissues in comparison to NE tissues (Fig. 3A). Subsequently, real-time PCR and ELISA assay demonstrated that PAX2 expression was markedly elevated in all 20 patients in comparison to NE tissues (Fig. 3B, C). The results presented herein demonstrate that PAX2 is expressed at a high level in EC tissues. Furthermore, we confirmed the expression of the target genes CD133, which may be regulated by PAX2 in the endometrium. Immunofluorescence and immunehistochemical staining demonstrated that CD133 was markedly expressed in EC tissues (Fig. 4A and B). Additionally, the expression of CD133 was investigated in 20 NE tissues and 20 EC tissues through the utilisation of real-time PCR and ELISA. The findings revealed a notable elevation in CD133 expression levels in EC tissues relative to NE tissues (Fig. 4C and D). The results demonstrated that the expression of CD133 was significantly increased in endometrial cells following carcinogenesis, it suggests a potential role for CD133 in the development of EC, in conjunction with PAX2. It was therefore investigated whether PAX2 plays a role in regulating CD133 expression. The results demonstrated that the overexpression of PAX2 in HEC-1A cells led to a significant increase in CD133 levels, the downregulation of PAX2 in HEC-1A cells led to a significant decrease in CD133 levels (Fig. 4E and F). Luciferase double-labelling experiments demonstrated that transfection of a CD133 luciferase reporter gene expression plasmid in PAX2-expressing HEC-1A cells resulted in the absence of CD133 expression when fragments of the promoter region of PAX2-bound CD133 were disrupted in the plasmid, leading to the non-detection of luciferin (Fig. 4G). The aforementioned results indicate that PAX2 can promote CD133 expression by binding to the promoter region of CD133, thereby facilitating CD133 expression. Therefore, it remains

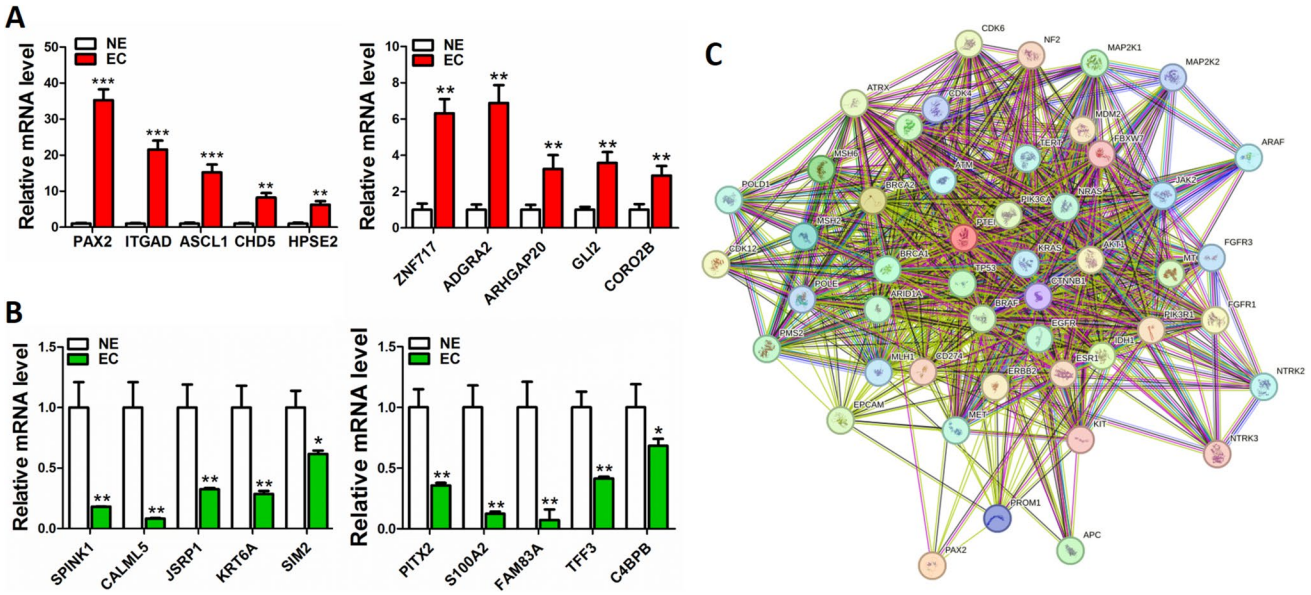


**Fig. 2** Verification of the RNA-sequence's high and low expression genes was achieved through real-time PCR (Top 10). **A** The top ten highly expressed genes were validated in real-time PCR, which yielded consistent results with the RNA-sequencing data. All genes were found to be significantly up-regulated in EC tissue. **B** Top 10 low expression genes were verified by real-time PCR, all genes were found to be significantly down-regulated in EC tissue. **C** PPI analyses indicated the existence of a potential regulatory relationship between the PAX2 and PROM1 proteins, although this requires further validation. *: vs control, **: $p < 0.01$

to be confirmed whether the role of PAX2 in promoting EC progression is achieved by its possible target protein, CD133.

## Tumourigenicity of HEC-1A cells with PAX2 interference is reduced in nude mice

The study employed a subcutaneous inoculation of HEC-1A cells transfected with the PAX2 interference plasmid in nude mice. The control group consisted of nude mice inoculated with negative control plasmid-transfected HEC-1A cells, allowing for the observation of the effect of PAX2 on tumour formation in nude mice. The findings of the study demonstrated a notable reduction in the tumourigenic weight and volume of HEC-1A cells that had been exposed to PAX2, in comparison to the control group (Fig. 5A, B, C). It demonstrates that interference with PAX2 results in a substantial reduction of the tumour-inducing properties of EC cells. The HE staining results clearly showed that the HEC-1A cell-derived nude mouse tumour-forming tissues exhibited the pathomorphological characteristics of endometrial cancer tissues. Furthermore, the morphology of the tumour tissues was observed to improve when PAX2 was interfered with in HEC-1A cells (Fig. 5D). Immunohistochemical staining of nude mouse tumour-forming tissues for PAX2 revealed a substantial number of PAX2-positive cells in the control tumour tissues (Fig. 5E). Concurrently, we investigated the expression of PAX2 and CD133 in tumourigenic tissues of nude mice and observed a notable reduction in the expression of PAX2 and CD133 in the tumourigenic tissues of HEC-1A cells that interfered with PAX2, in comparison to the control group (Fig. 5F–H). The aforementioned results demonstrated that the inhibition of PAX2 impeded the formation and progression of EC, as well as the expression of CD133 in these tissues. Consequently, we will undertake a comprehensive investigation into the regulatory mechanism of PAX2-targeted CD133 in EC formation.

## Interference with CD133 inhibits the promotion of EC formation by PAX2

The initial objective was to examine the effects of PAX2 on the proliferation, adhesion, migration and apoptosis of EC cells. Our findings demonstrated that PAX2 overexpression increased the proliferation potential of HEC-1A cells (Fig. 6A). In addition, it was demonstrated that interference with PAX2, or the addition of the PAX2 inhibitor EG1, resulted in a significant decrease in adhesion capacity (Fig. 6B), the migration ability (Fig. 6C) and the invasion ability (Fig. 6D) of HEC-1A cells. Furthermore, interference with PAX2, or the addition of the PAX2 inhibitor EG1, resulted in a significant increase in the apoptosis of HEC-1A cells (Fig. 6E). The results suggest that PAX2 promotes the proliferation, migration, invasion, and adhesion of EC cells while inhibiting their apoptosis. Subsequently, the impact of recombinant human PAX2 protein on CD133-interfering HEC-1A cells was investigated

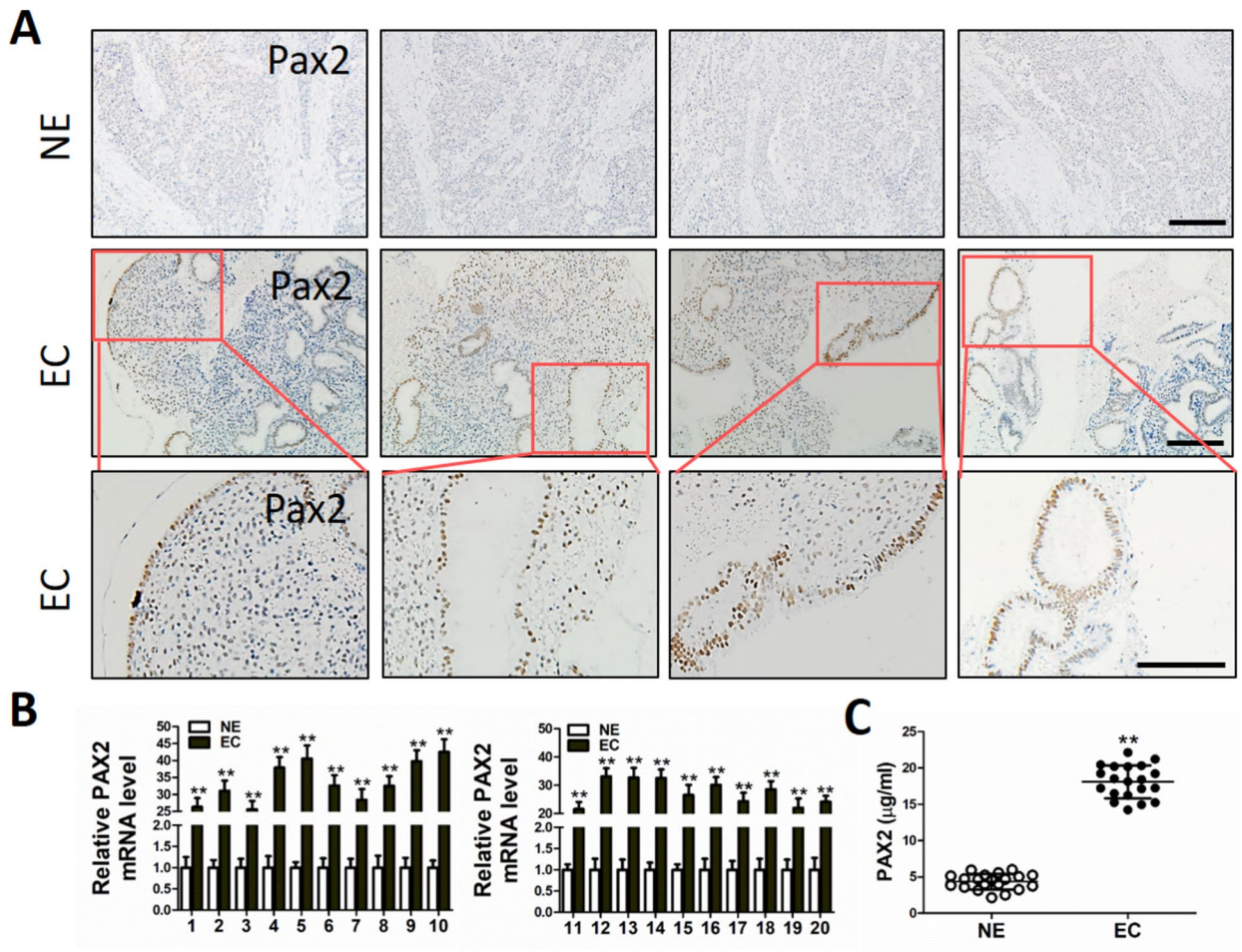


**Fig. 3** Expression of PAX2 in EC tissues. **A** Immunohistochemical staining confirmed the high expression of PAX2 in EC tissues. **B** Real-time PCR examined the PAX2 mRNA level in all 20 patients with EC, results showed that PAX2 was significantly higher in EC tissues. **C** Elisa revealed a significantly greater PAX2 protein in the 20 EC tissues than in the typical endometrial tissue. *: vs control, **: $p < 0.01$. Scale bar, 50 μm or 100 μm

to substantiate its function in facilitating EC progression. The results indicate that recombinant human PAX2 protein did not promote the proliferation (Fig. 6F), adhesion (Fig. 6G), migration (Fig. 6H), or invasion (Fig. 6I) of HEC-1A cells that were interfered with CD133, additionally, PAX2 also failed to inhibit the apoptosis of HEC-1A cells that were interfered with CD133 (Fig. 6J). These results confirm that CD133 plays a pivotal role in the progression of EC and represents a key target for PAX2.

## Interference with CD133 affects the regulation of mitochondrial function in EC cells by PAX2

What is the mechanism of action of PAX2 in targeting CD133 to promote EC progression? We monitored the metabolic dynamics of HEC-1A cells by assessing mitochondrial function, considering the influence of cellular metabolism on EC cell status. The mitochondrial function and glycolytic activity of EC cells were evaluated by measuring the oxygen consumption rate (OCR) and extracellular acidification rate (ECAR), respectively. The results showed that down-regulated CD133 expression increased oxidative phosphorylation (Fig. 7A) and decreased glycolysis (Fig. 7B). In contrast, rhPAX2 decreased oxidative phosphorylation and increased glycolysis. When rhPAX2 was added to cells interfering with CD133, it was found that CD133 inhibited the promotion of oxidative phosphorylation by PAX2 (Fig. 7C), while reducing the inhibition of glycolysis by PAX2 (Fig. 7D). The aforementioned results indicate that CD133 plays a pivotal role in the metabolic transition of EC cells from oxidative phosphorylation to glycolysis. We further evaluated the effects of PAX2 and CD133 on mitochondrial function by examining mitochondrial copy number, ROS, hexokinase, and mitochondrial calcium ion concentration. The results indicate that both PAX2 and CD133 increased mitochondrial copy number, ROS, hexokinase, and calcium ion levels. However, the elevation of PAX2 expression levels

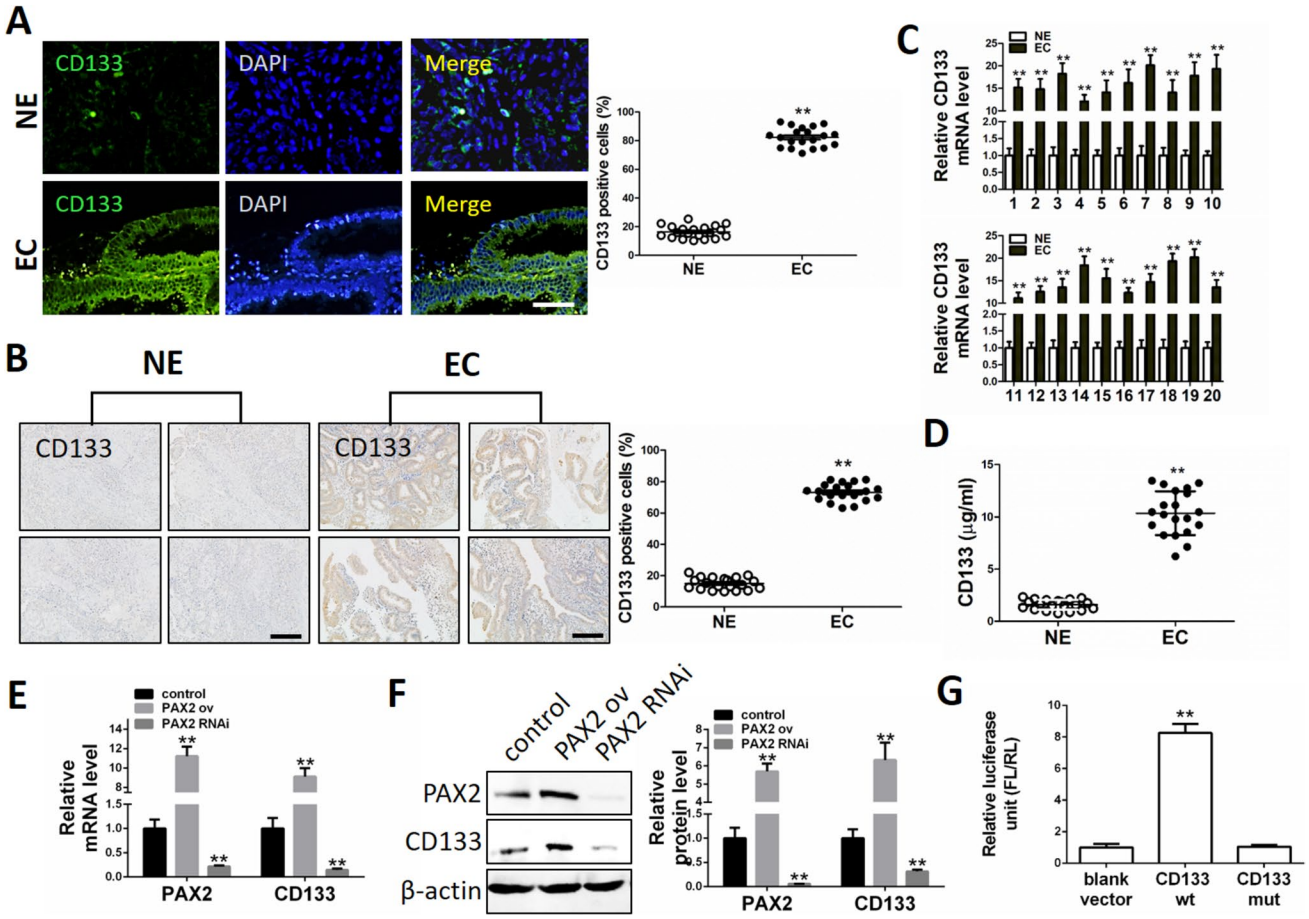


**Fig. 4** Expression of PAX2 target genes CD133 in EC tissues. **A** The results of the immunofluorescence staining demonstrated a markedly elevated fluorescence intensity of CD133 in EC tissues when compared to the controls. **B** 4 EC cases revealed a higher CD133 expression level than in typical endometrial tissues. **C** Real-time PCR results showed that CD133 was highly expressed in EC tissues (20 cases) compared with NE tissues (20 cases). **D** Elisa demonstrated that CD133 was markedly expressed in EC tissues (20 cases) in comparison to NE tissues (20 cases). **E–F** Overexpression of PAX2 in HEC-1A cells significantly increased the level of PAX2 and CD133, the simultaneous inhibition of PAX2 and CD133 expression levels was observed following the interference with PAX2. **H** The dual-luciferase reporter gene assay demonstrates that PAX2 is unable to induce CD133 expression following interference with the CD133 promoter. *: vs control, **: $p < 0.01$. Scale bar, 50 μm or 100 μm

was significantly suppressed when CD133 expression was interfered with in EC cells (Fig. 7E–H). The results indicate that PAX2 and CD133 affect mitochondrial function and contribute to the progression of EC. PAX2 affects EC progression through mitochondrial function less when CD133 is lower.

## CD133 affects mitochondrial function in EC cells through activation of AKT1

We analysed the relationships between PAX2, CD133 and AKT1 and their relationships with proteins that regulate mitochondrial function using PPI and found that PAX2-CD133 may influence cellular mitochondrial function through AKT1 (Fig. 8A). An investigation was therefore conducted into the phosphorylation of AKT1 in 20 normal human endometrial tissues and 20 EC tissues. The results of this investigation revealed that the protein AKT1 was found to be highly phosphorylated in EC tissues (Fig. 8B). The results obtained suggest that the process of AKT1 phosphorylation may be subject to regulation by the PAX2-CD133 pathway. Nude mouse tumour-forming tissue and HEC-1A cells and found that in the uterus, the phosphorylation level of AKT1 was increased in EC tissue and decreased in HEC-1A cells that interfered with PAX2 or CD133, suggesting that PAX2-CD133 is involved in regulating AKT1 phosphorylation. Furthermore, we investigated the phosphorylation status of AKT1 in the tumour-forming tissues of HEC-1A nude mice. Our findings revealed a notable reduction in AKT1 phosphorylation levels in the tumour-forming tissues of HEC-1A cells that had been interfered with PAX2, as compared to HEC-1A cells that had not been interfered with PAX2 (Fig. 8C). Concurrently, we observed

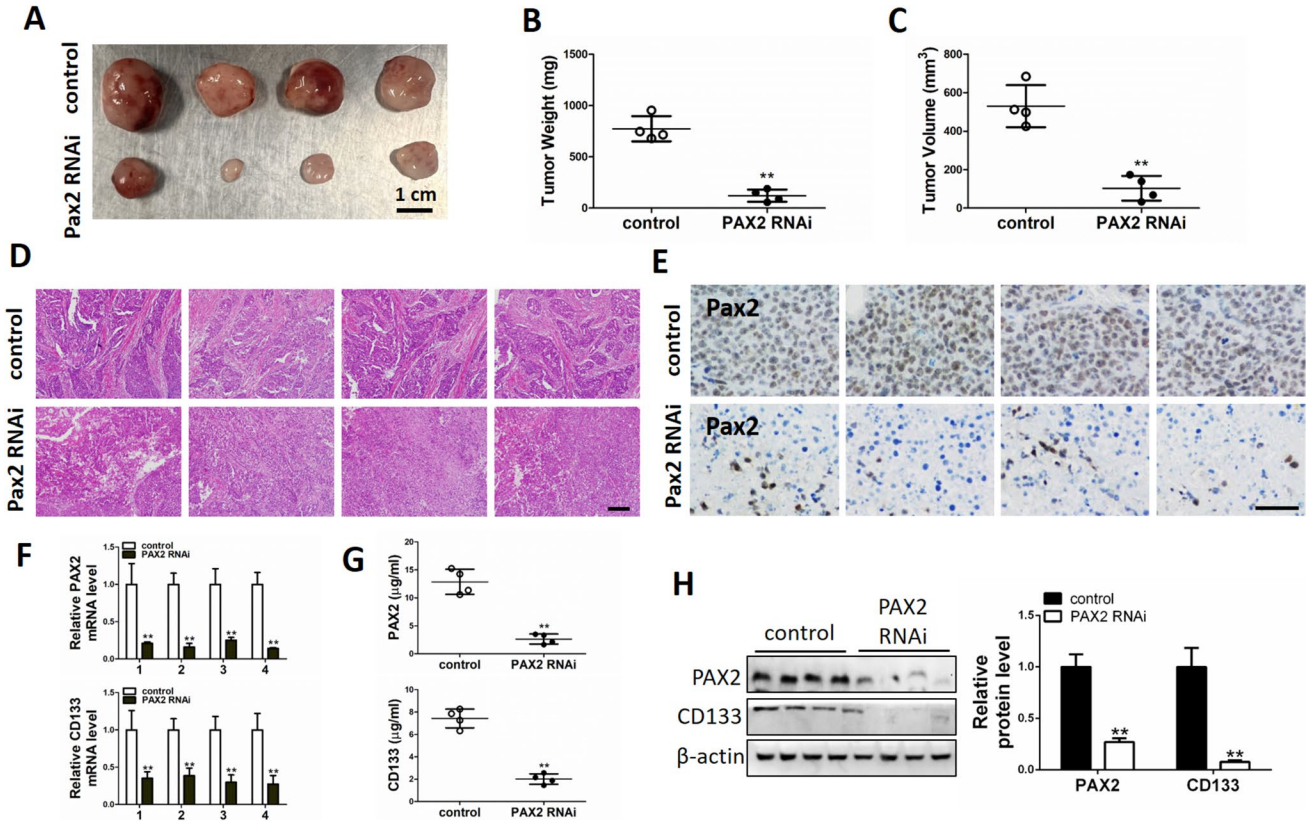


**Fig. 5** PAX2 interferes with tumour formation in HEC-1A cells in nude mice. **A** Demonstration of HEC-1A cell tumour-forming tissues in nude mice. **B** Inhibition of PAX2 in HEC-1A cells has been demonstrated to result in a notable reduction in the weight of tumours in nude mice. **C** Inhibition of PAX2 in HEC-1A cells has been demonstrated to result in a notable reduction in the volume of tumours in nude mice. **D** The HE staining demonstrates the histopathological morphology of tumour-forming tissues in nude mice. **E** The immunohistochemical staining for PAX2 demonstrated that PAX2 was markedly expressed in the control group. **F–G** The results of the real-time PCR and ELISA assays demonstrated that the expression of PAX2 and CD133 in the tumour-forming tissues of the cellular nude mice that did not receive PAX2 intervention was markedly higher than that observed in the intervention group. **H** WB assay confirms significant reduction of PAX2 and CD133 in tumourigenic tissues of nude mice interfering with PAX2 compared to controls. *: vs control, **: $p < 0.01$

the phosphorylation of AKT1 in HEC-1A cells, which resulted in the interference of PAX2 and CD133. Furthermore, we found that the phosphorylation level of AKT1 in the cells was significantly reduced in both interfered cells when compared with the normal control (Fig. 8D, E). The results presented herein demonstrate that the protein PAX2 can promote the phosphorylation of AKT1 by increasing the expression of CD133.

The subsequent step was to ascertain whether CD133 exerts an influence on mitochondrial functionality via AKT1. The results demonstrated that the inhibition of AKT1 promoted oxidative phosphorylation and inhibited glycolysis in HEC-1A cells (Fig. 9A, B). The addition of recombinant CD133 to HEC-1A cells in which AKT1 was inhibited did not result in a reduction in oxidative phosphorylation or an increase in glycolysis (Fig. 9C, D). The results demonstrated that following interference with AKT1, CD133 lost its regulatory function in relation to mitochondrial function. In order to further observe the effect of AKT1 on mitochondrial function and whether CD133 affects mitochondrial function by promoting AKT1 phosphorylation, we examined mitochondrial function-related indicators. Agonists of AKT1 were observed to significantly elevate the quantity of mitochondrial DNA, the level of ROS, hexokinase, and the level of calcium ions. Conversely, the inhibition of AKT1 resulted in a significant decrease in the aforementioned mitochondrial function indexes. Furthermore, the addition of recombinant CD133 was unable to elevate the level of mitochondrial function through AKT1. Additionally, recombinant CD133 was ineffective in enhancing mitochondrial function in HEC-1A cells (Fig. 9E–H). Our findings demonstrate that PAX-CD133 plays a role in EC development by regulating AKT1 phosphorylation and influencing mitochondrial function in endometrial cancer cells (Fig. 10).

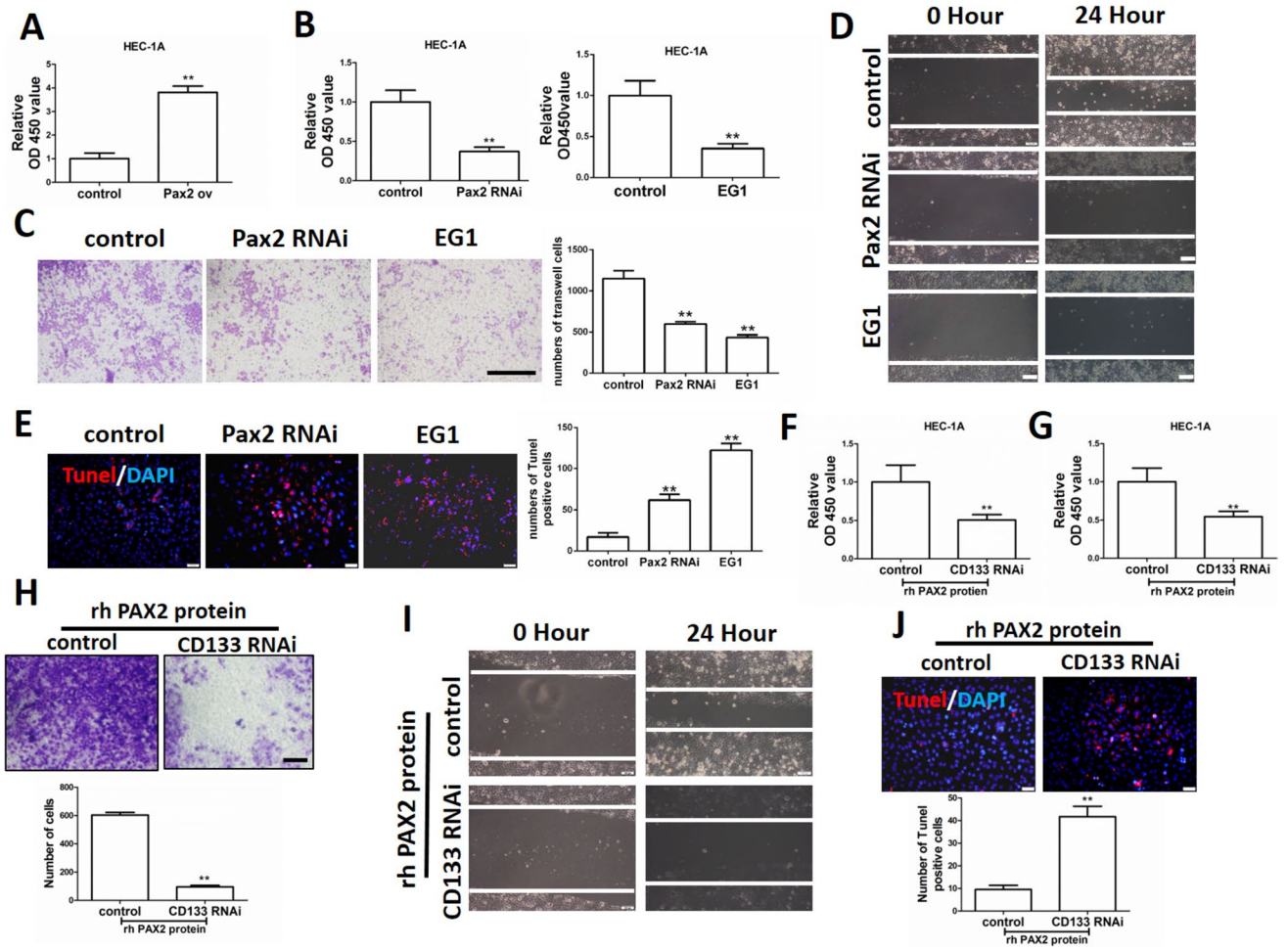


**Fig. 6** Interference with CD133 inhibited the role of PAX2 in promoting EC. **A** Overexpression of PAX2 in HEC-1A cells promotes cell proliferation. **B** It was demonstrated that interference with PAX2 in HEC-1A cells or the addition of the PAX2 inhibitor EG1 resulted in a significant inhibition of cell adhesion. **C** Interference with PAX2 or the addition of the PAX2 inhibitor EG1 in HEC-1A cells inhibits cells migration. **D** Interference with PAX2 or the addition of the PAX2 inhibitor EG1 in HEC-1A cells inhibits cells invasion. **E** PAX2 RNAi or the addition of the PAX2 inhibitor EG1 promotes HEC-1A cells apoptosis. **F** Recombinant human PAX2 protein (rh PAX2 protein) did not promote the proliferation of HEC-1A cells that interfered with CD133. **G** rh PAX2 protein failed to promote HEC-1A cell adhesion that interfered with CD133. **H** rh PAX2 protein failed to promote HEC-1A cell migration that interfered with CD133. **I** rh PAX2 protein failed to promote HEC-1A cell invasion that interfered with CD133. **J** rh PAX2 protein also failed to inhibit the apoptosis of HEC-1A cells that interfered with CD133.*: vs control, **: $p < 0.01$. Scale bar, 50 μm or 100 μm or 200 μm

## Discussion

The European Society of Gynecological Oncology Guidelines of 2017 advise the employment of PAX2 immunohistochemistry to detect precancerous endometrial hyperplasia [19]. Studies have shown that PAX2 hypomethylation mediates the development of tamoxifen-stimulated EC, and the study found that tamoxifen and estrogen have different but overlapping target gene profiles, and among these overlapping target genes, the authors identified a pair of box-like genes, PAX2, which plays a crucial role in cell proliferation and carcinogenesis in the EC: PAX2 is activated by estrogen and tamoxifen in EC, but no activation of PAX2 is found in normal endometrium. The study showed that estrogen-associated EC must be accompanied by PAX2 activation, which is associated with reduced methylation levels in the PAX2 promoter region [20]. Studies have shown that PAX2 plays a key role in cell fate, early modeling, and organ formation. Regarding the mechanism of PAX2 in regulating the pathogenesis of EC, some studies have found that PAX2 plays an important role in the occurrence of EC by affecting the expression of cyclin-dependent kinase 1 (CDK1), promoting the proliferation and enhancing the mobility of EC cells [21]. Studies have evaluated whether PAX2 expression can predict progression-free

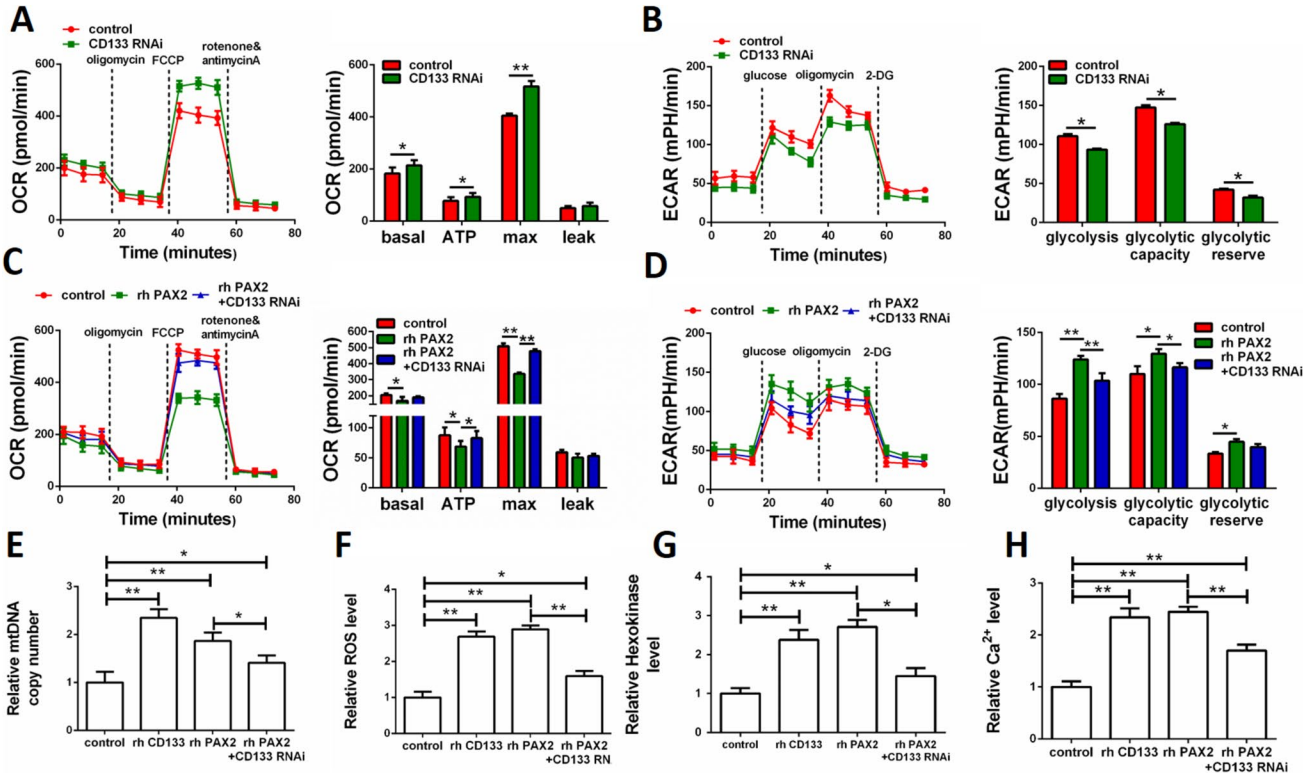


**Fig. 7** PAX2 promotes mitochondrial dysfunction target CD133 in EC. **A** Results of OCR showed that CD133 inhibited oxidative phosphorylation in HEC-1A cells. **B** Results of ECAR showed that CD133 promoted glycolysis in HEC-1A cells. **C** Inhibition of oxidative phosphorylation by PAX2 in HEC-1A cells is attenuated after interference with CD133. **D** Promotion of glycolysis by PAX2 in HEC-1A cells is attenuated after interference with CD133. **E–H** The promotion of mitochondrial DNA increase, elevated ROS, elevated hexokinase and elevated mitochondrial calcium ion concentration by PAX2 in HEC-1A cells was attenuated after interfering with CD133. *: vs control, **: $p < 0.01$. Scale bar, 50 μm or 100 μm

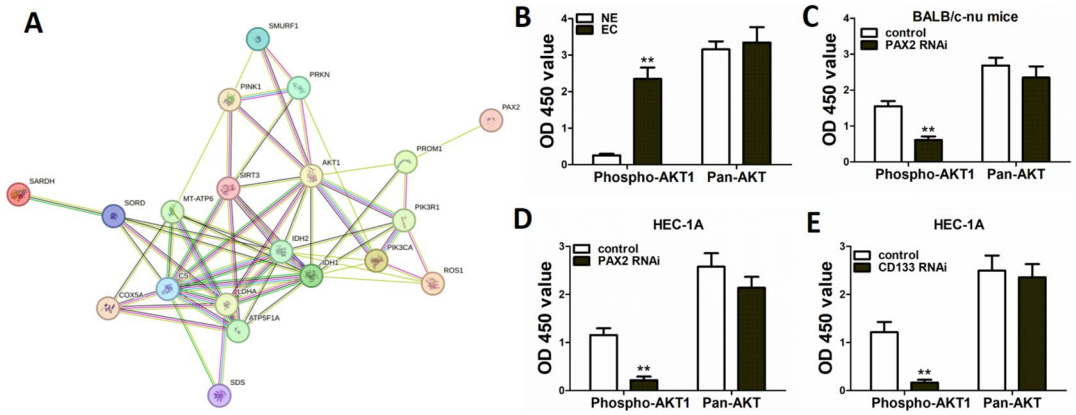


**Fig. 8** Verification that CD133 affects mitochondrial function through the AKT1 pathway. **A** PPI analysis of PAX2, CD133 and AKT1 in relation to mitochondrial function-related proteins. **B** Elisa indicated that there was an increase in AKT1 phosphorylation levels in EC tissues in comparison to NE tissues. **C** Elisa detection of AKT1 phosphorylation level in tumour-forming tissues of nude mice, the expression of phosphorylated AKT1 is markedly diminished following the interference of PAX2. **D** Elisa indicated that there was a decrease in AKT1 phosphorylation levels in HEC-1A cells interfering with PAX2. **E** Elisa indicated that there was a decrease in AKT1 phosphorylation levels in HEC-1A cells interfering with CD133. *: vs control, **: $p < 0.01$

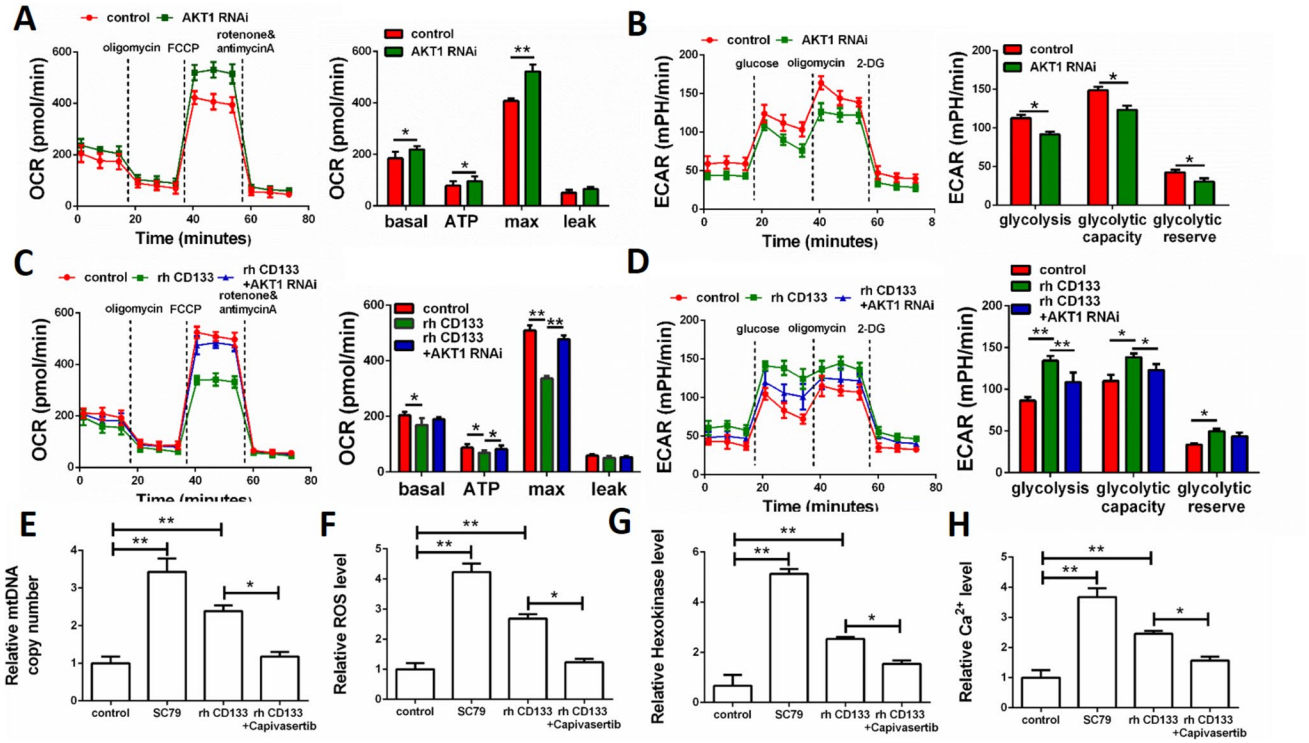


**Fig. 9** CD133 affects mitochondrial function through the AKT1 pathway. **A** Results of OCR showed that AKT1 inhibited oxidative phosphorylation in HEC-1A cells. **B** Results of ECAR showed that AKT1 promoted glycolysis in HEC-1A cells. **C** Inhibition of oxidative phosphorylation by CD133 in HEC-1A cells is attenuated after interference with AKT1. **D** Promotion of glycolysis by CD133 in HEC-1A cells is attenuated after interference with AKT1. (**E**–**H**) The promotion of mitochondrial DNA increase, elevated ROS, elevated hexokinase and elevated mitochondrial calcium ion concentration by CD133 in HEC-1A cells was attenuated after interfering with AKT1. *: vs control, **: $p < 0.01$. Scale bar, 50 μm or 100 μm

survival of endometrial intraepithelial neoplasia and EC. Progression-free survival analysis showed that patients with high risk of endometrial intraepithelial neoplasia with PAX2 expression score (h score ≤ 75) had a higher probability of disease progression compared with patients with low risk score (h score > 75). PAX2 expression was not associated with prognosis in EC [22]. Studies have also examined the expression of PAX2 in proliferative and malignant endometrium, as well as proliferative and atrophic endometrium, and found that with the progression of tumor lesions from precancerous state to EC, PAX2 expression increases, suggesting that PAX2 may promote the development of EC. These contrary findings reinforce the need to clarify the role of PAX2 in EC. The research content of PAX2 in other types of tumors such as ovarian cancer, kidney and nerve cell diseases is very rich [23, 24]. Our results showed that compared with NE tissues, PAX2 expression was significantly increased in EC tissues, and PAX2 was found to affect the occurrence and development of EC by regulating CD133.

CD133 is a five-transmembrane glycoprotein that is also one of the most well-known markers of tumor stem cells. CD133-positive cells play an important role in tumorigenesis, metastasis, recurrence and drug resistance [25]. CD133-positive cells isolated in EC tissue were able to initiate tumor formation and reproduce the phenotype of the primary tumor [26]. The above study help us to understand the mechanism of endometrial regeneration and EC occurrence, and help to establish a new molecular basis for cancer therapy targeting stem cells, CD133 has become an important target protein for the study of EC. Studies have shown that CD133 is expressed in 87.09% of EC, which is significantly different from the normal group, and CD133 is expressed more in early tumors (FIGO stage I–II) than in FIGO stage III–IV [27]. Xenotransplantation experiments in nude mice further showed that CD133 + cells had higher tumorigenic ability than CD133- cells, indicating that CD133 + cells had tumorigenic ability [28]. Although CD133 is currently used as a tumor stem cell marker, its exact physiological function is still unknown, and its ubiquitous presence indicates its importance. CD133's capacity to control the expression of vascular endothelial growth factor (VEGF), a protein involved in neovascularization and angiogenesis [29] has been discovered. Furthermore, CD133-positive cells have been found to upregulate FLIP, a FLIS-like inhibitory protein, in

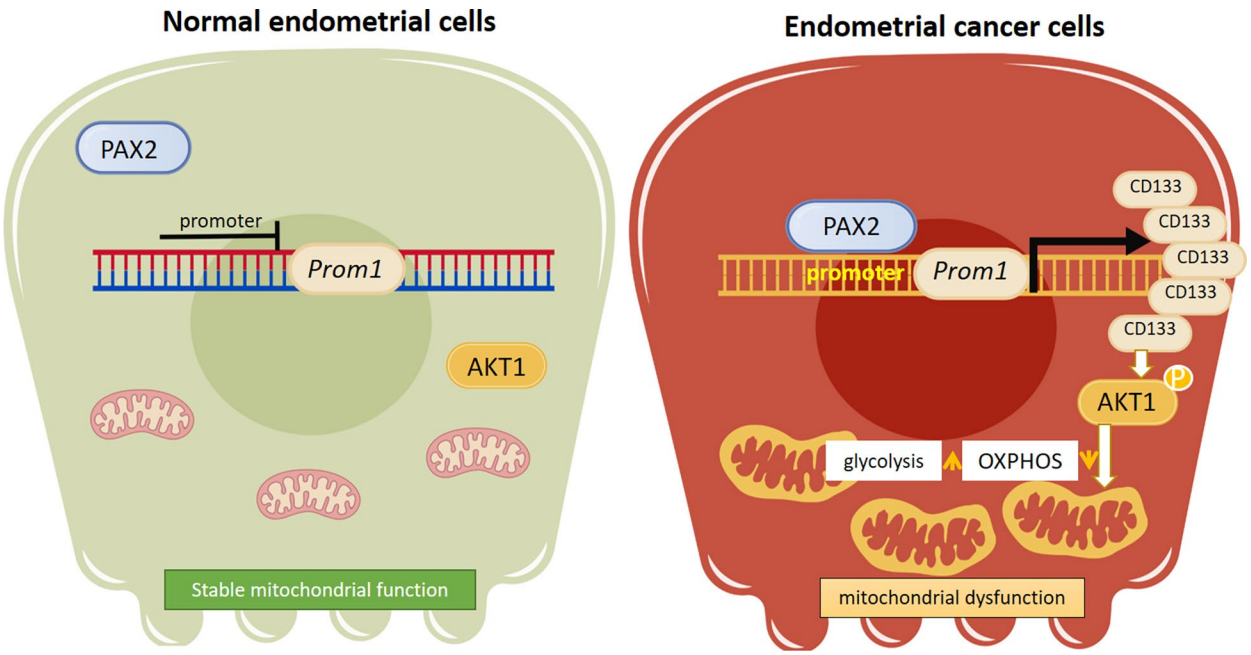


**Fig. 10** schema diagram. In normal endometrial cells, PAX2 is found in the cytoplasm and is not involved in the transcriptional regulation of the *PROM1* gene. Consequently, AKT in the cytoplasm is not phosphorylated and thus does not alter cellular mitochondrial function. In the context of EC cells, PAX2 has been observed to bind to the promoter region of the *PROM1* gene, thereby promoting the expression of the PAX2 gene. Furthermore, these cells have been found to express a significant amount of CD133 protein, which in turn promotes the phosphorylation of AKT1. This, in turn, results in a decrease in the level of oxidative phosphorylation of the cellular mitochondria and an increase in the level of glycolysis. This, in turn, promotes the dysfunction of the mitochondria, thus inducing the development of EC

order to inhibit apoptosis caused by tumor necrosis factor α (TNF-α)-associated apoptosis-inducing ligand (TRAIL) [30]. Study also found that mitochondrial uncoupling is a metabolic feature of CD133(+) colon cancer cells that provides protection against piperlongumine therapy by suppressing mitochondrial ROS generation [30], and CD133 acts to maintain mitochondrial function through its interaction with ND20 which is active in the mitochondrial electron transport chain [31]. In conclusion, existing studies have shown that CD133 maintains the characteristics of tumor stem cells by regulating various pathways that promote tumorigenesis, and promotes the proliferation, migration and drug resistance of tumor cells. Therefore, it is important to clarify the regulatory relationship between PAX2 and CD133 for further study of the pathogenesis of EC. Through the use of PPI network analysis, we have identified a potential regulatory relationship between PAX2 and CD133. Our findings indicate that both PAX2 and CD133 are highly expressed in EC tissues. In vitro studies have shown that PAX2 promotes the proliferation, adhesion, migration, and invasion of EC cells. However, these functions were weakened in EC cells where CD133 was interfered with. Mitochondria are the main source of energy provided by the cell. Most cancer cells retain mitochondrial functions, including respiration. Some tumour cells retain high levels of oxidative phosphorylation, while other tumour cells that use glycolysis for energy still retain mitochondrial respiration and other functions [32]. We found that interfering with CD133 in EC cells elevated cellular oxidative phosphorylation levels while decreasing glycolysis levels, suggesting that CD133 promotes tumour progression by increasing cellular glycolysis. In contrast, administration of rhPAX2 to EC cells increased the level of oxidative phosphorylation and inhibited the glycolysis process, a phenomenon that was altered after interfering with CD133, suggesting that PAX2 affects the mitochondrial function of cells via CD133 and thus promotes the progression of EC. Nevertheless, further investigation is required to elucidate the precise regulatory mechanism by which PAX2-CD133 promotes endometrial cancer progression.

It has been demonstrated that the expression of AKT1 in EC tissues is markedly elevated in comparison to that observed in NE tissues [33]. AKT1 plays a pivotal role in the regulation of cell growth, proliferation and survival, primarily through the phosphorylation of a diverse range of downstream substrates, including mTOR and 4E-BP1 [34]. In endometrial cancer, the over-activation of AKT1 may result in abnormalities within these downstream signalling pathways, which in turn promote cancer cell growth and invasion. Given the pivotal role of AKT1 in endometrial

cancer, the development of drugs targeting AKT1 and its associated pathways has emerged as a prominent area of research [35]. For example, capivasertib, an AKT1 inhibitor, has demonstrated therapeutic efficacy in clinical trials for patients with advanced tumours carrying AKT1 mutations [36]. It is therefore important to further explore the specific mechanism of action of AKT1 in EC, with a particular focus on how it interacts with other signalling pathways to regulate the growth and invasion of cancer cells. Our findings indicate that the PAX2-CD133 pathway accelerates the progression of EC by promoting AKT1 phosphorylation, inhibiting oxidative phosphorylation in EC cells, promoting glycolysis, increasing mitochondrial copy number, and elevating ROS, hexokinase, and calcium ion levels.

**Author contributions** YLC crafted the experiments, revised the manuscript, and FH scrutinized and comprehended the data, created the manuscript, and contributed to the molecular, cellular, and animal experiments. All the authors concurred and ratified the ultimate manuscript.

**Funding** Grants from the Natural Science Foundation of China (program no. 6590000258) provided backing for this study.

**Data availability** The original contributions presented in the study are included in this article, further inquiries can be directed to the corresponding author.

## Declarations

**Conflict of interest** Declaring that no commercial or financial ties could be seen as a possible conflict of interest, the authors assert that the research was conducted without any such connections.

**Ethical approval** Patients have signed informed consent. The project was approved by Jiangsu Province Health and Health Committee (No. H2021067) (20210101-20221231), applied by the Department of Gynecology, the Affiliated Huaian No. 1 People's Hospital of Nanjing Medical University. Doctor FuHua, had submitted relevant ethical approval before the project application and obtained ethical qualifications. The animal study was reviewed and approved by the Animal Care Committee for the use of laboratory animals at the DongNan University.



## References

1. Morice P et al (2016) Endometrial cancer. Lancet 387(10023):1094–1108
2. Siegel RL, Miller KD, Jemal A (2018) Cancer statistics, 2018. CA Cancer J Clin 68(1):7–30
3. Henley SJ et al (2020) Annual report to the nation on the status of cancer, part I: national cancer statistics. Cancer 126(10):2225–2249
4. Colombo N et al (2016) ESMO-ESGO-ESTRO Consensus conference on endometrial cancer: diagnosis, treatment and follow-up. Ann Oncol 27(1):16–41
5. Jahangiri R et al (2018) PAX2 expression is correlated with better survival in tamoxifen-treated breast carcinoma patients. Tissue Cell 52:135–142
6. Jahangiri R et al (2022) PAX2 promoter methylation and AIB1 overexpression promote tamoxifen resistance in breast carcinoma patients. J Oncol Pharm Pract 28(2):310–325
7. Johnson SA et al (2011) Discrete regulatory regions control early and late expression of D-Pax2 during external sensory organ development. Dev Dyn 240(7):1769–1778
8. McDaniel AS et al (2016) A subset of solitary fibrous tumors express nuclear PAX8 and PAX2: a potential diagnostic pitfall. Histol Histopathol 31(2):223–230
9. Aguilar M et al (2022) Reliable identification of endometrial precancers through combined Pax2, beta-catenin, and pten immunohistochemistry. Am J Surg Pathol 46(3):404–414
10. Alwosaibai K et al (2022) PAX2 induces vascular-like structures in normal ovarian cells and ovarian cancer. Exp Ther Med 23(6):412
11. Yang S et al (2023) Role of PAX2 in breast cancer verified by bioinformatics analysis and in vitro validation. Ann Transl Med 11(2):58
12. Ueda T et al (2015) PAX2 promoted prostate cancer cell invasion through transcriptional regulation of HGF in an in vitro model. Biochim Biophys Acta 1852(11):2467–2473
13. Huang B et al (2012) WT1 and Pax2 re-expression is required for epithelial-mesenchymal transition in 5/6 nephrectomized rats and cultured kidney tubular epithelial cells. Cells Tissues Organs 195(4):296–312
14. Wu H et al (2005) Hypomethylation-linked activation of PAX2 mediates tamoxifen-stimulated endometrial carcinogenesis. Nature 438(7070):981–987
15. Pattipaka S et al (2022) Magneto-mechano-electric (MME) composite devices for energy harvesting and magnetic field sensing applications. Sensors (Basel) 22(15):5723
16. Porporato PE et al (2018) Mitochondrial metabolism and cancer. Cell Res 28(3):265–280
17. Gross SM, Rotwein P (2016) Mapping growth-factor-modulated Akt signaling dynamics. J Cell Sci 129(10):2052–2063
18. Samakova A et al (2019) The PI3k/Akt pathway is associated with angiogenesis, oxidative stress and survival of mesenchymal stem cells in pathophysiologic condition in ischemia. Physiol Res 68(Suppl 2):S131–S138
19. Raffone A et al (2019) PAX2 in endometrial carcinogenesis and in differential diagnosis of endometrial hyperplasia: a systematic review and meta-analysis of diagnostic accuracy. Acta Obstet Gynecol Scand 98(3):287–299
20. Wang J et al (2018) Paired box 2 promotes progression of endometrial cancer via regulating cell cycle pathway. J Cancer 9(20):3743–3754
21. Jia N et al (2016) DNA methylation promotes paired box 2 expression via myeloid zinc finger 1 in endometrial cancer. Oncotarget 7(51):84785–84797

22. Monte NM et al (2010) Joint loss of PAX2 and PTEN expression in endometrial precancers and cancer. Cancer Res 70(15):6225–6232
23. Saida K et al (2020) A novel truncating PAX2 mutation in a boy with renal coloboma syndrome with focal segmental glomerulosclerosis causing rapid progression to end-stage kidney disease. CEN Case Rep 9(1):19–23
24. Lv N et al (2021) The role of PAX2 in neurodevelopment and disease. Neuropsychiatr Dis Treat 17:3559–3567
25. Grabovenko FI et al (2022) Protein CD133 as a tumor stem cell marker. Zh Vopr Neirokhir Im N N Burdenko 86(6):113–120
26. Ding DC et al (2017) Expression of CD133 in endometrial cancer cells and its implications. J Cancer 8(11):2142–2153
27. Shang C, Lang B, Meng LR (2018) Blocking NOTCH pathway can enhance the effect of EGFR inhibitor through targeting CD133+ endometrial cancer cells. Cancer Biol Ther 19(2):113–119
28. Grosse-Gehling P et al (2013) CD133 as a biomarker for putative cancer stem cells in solid tumours: limitations, problems and challenges. J Pathol 229(3):355–378
29. Li X et al (2019) Premobilization of CD133+ cells by granulocyte colony- stimulating factor attenuates ischemic acute kidney injury induced by cardiopulmonary bypass. Sci Rep 9(1):2470
30. Lee JH et al (2022) CD133 increases oxidative glucose metabolism of HT29 cancer cells by mitochondrial uncoupling and its inhibition enhances reactive oxygen species-inducing therapy. Nucl Med Commun 43(8):937–944
31. Wang X et al (2019) Drosophila prominin-like, a homolog of CD133, interacts with ND20 to maintain mitochondrial function. Cell Biosci 9:101
32. Zong WX, Rabinowitz JD, White E (2016) Mitochondria and cancer. Mol Cell 61(5):667–676
33. Huo X et al (2019) Clinical and expression significance of AKT1 by Co-expression network analysis in endometrial cancer. Front Oncol 9:1147
34. Trigka EA et al (2013) A detailed immunohistochemical analysis of the PI3K/AKT/mTOR pathway in lung cancer: correlation with PIK3CA, AKT1, K-RAS or PTEN mutational status and clinicopathological features. Oncol Rep 30(2):623–636
35. Chen J et al (2014) Activation of PI3K/Akt/mTOR pathway and dual inhibitors of PI3K and mTOR in endometrial cancer. Curr Med Chem 21(26):3070–3080
36. Turner NC et al (2023) Capivasertib in hormone receptor-positive advanced breast cancer. N Engl J Med 388(22):2058–2070